Use the template dedic.tex *together with the Springer document class SVMono for monograph-type books or SVMult for contributed volumes to style a quotation or a dedication at the very beginning of your book in the Springer layout*

Foreword

Use the template *foreword.tex* together with the Springer document class SVMono (monograph-type books) or SVMult (edited books) to style your foreword in the Springer layout.

The foreword covers introductory remarks preceding the text of a book that are written by a *person other than the author or editor* of the book. If applicable, the foreword precedes the preface which is written by the author or editor of the book.

Place, month year *Firstname Surname*

Preface

Use the template *preface.tex* together with the Springer document class SVMono (monograph-type books) or SVMult (edited books) to style your preface in the Springer layout.

A preface is a book's preliminary statement, usually written by the *author or editor* of a work, which states its origin, scope, purpose, plan, and intended audience, and which sometimes includes afterthoughts and acknowledgments of assistance.

When written by a person other than the author, it is called a foreword. The preface or foreword is distinct from the introduction, which deals with the subject of the work.

Customarily *acknowledgments* are included as last part of the preface.

Place(s),
month year

Firstname Surname
Firstname Surname

Acknowledgements

Use the template *acknow.tex* together with the Springer document class SVMono (monograph-type books) or SVMult (edited books) if you prefer to set your acknowledgement section as a separate chapter instead of including it as last part of your preface.

Contents

List of Contributors

Mohit P. Dalwadi
Synthetic Biology Research Centre, University of Nottingham, University Park, Nottingham, NG7 2RD, UK, e-mail: mohit.dalwadi@nottingham.ac.uk

Acronyms

Use the template *acronym.tex* together with the Springer document class SVMono (monograph-type books) or SVMult (edited books) to style your list(s) of abbreviations or symbols in the Springer layout.

Lists of abbreviations, symbols and the like are easily formatted with the help of the Springer-enhanced `description` environment.

ABC	Spelled-out abbreviation and definition
BABI	Spelled-out abbreviation and definition
CABR	Spelled-out abbreviation and definition

Chapter 1
Asymptotic homogenization with a macroscale variation in the microscale

Mohit P. Dalwadi

Abstract Asymptotic homogenization is a useful mathematical tool that can be used to reduce the complexity of a problem with a periodic geometry. Generally, for asymptotic homogenization to be applicable, the full problem must have: (i) a periodic microstructure and (ii) a small ratio between the typical lengths of the periodic cell and the macroscale variation. In this Chapter we consider a model for drug delivery. Namely, we discuss an asymptotic homogenization for the concentration field of a drug diffusing within a domain that contains a near-periodic array of circular obstructions whose boundaries can absorb the drug. In particular, the radii of these circular obstructions can slowly vary in space, and thus the microscale geometry varies in the macroscale. Constraining the shape of the obstacles to a one-parameter family, where the only variation is circle radius, allows us to homogenize this problem in a computationally efficient manner. Moreover, the method we present allows us to determine the homogenized equation for any arrangement of the microstructure within the one-parameter constraint.

1.1 Introduction

Asymptotic homogenization can often be used to reduce the complexity of a problem that has a periodic geometry. Starting from the governing equations for the full problem, the general idea behind asymptotic homogenization is to obtain governing equations for the variables averaged over one periodic cell, and this lengthscale is referred to as the *microscale*. Determining the homogenized equations usually requires solving a given problem over one periodic cell, known as the *cell problem*. Solving the cell problem once and then solving the resulting homogenized equations is generally less computationally expensive than solving the full problem. This is

Mohit P. Dalwadi
Synthetic Biology Research Centre, University of Nottingham, University Park, Nottingham, NG7 2RD, UK, e-mail: mohit.dalwadi@nottingham.ac.uk

because the homogenization procedure has removed the periodic variation from the problem while retaining the slow change over many periodic cells, and this longer lengthscale is referred to as the *macroscale*. Asymptotic homogenization methods have been widely studied in the literature (see, for example, [2, 10, 11, 16, 19]).

We will consider asymptotic homogenization via the method of multiple scales [2] rather than, for example, volume averaging methods [19]. Generally, the assumptions required to apply the technique of asymptotic homogenization via the method of multiple scales are: (i) there is a periodic microstructure and (ii) the ratio between the length of the periodic cell and the length of the macroscale variation is small. An introduction to this method is given in Chapter **??**. In this Chapter, we see how to relax the assumption that the microstructure is strictly periodic, and we consider a microscale structure that varies over the macroscale.

1.1.1 Literature review

The method we consider in this Chapter to deal with a macroscopic variation in the microstructure has been applied to a wide variety of problems (see, for example, [3, 7, 8, 9, 12, 13, 14, 15, 17, 18]), and has formal analysis roots in, for example, [1, 5]. The general idea behind this method is to prescribe a level-set function to define the microstructure in both the microscale and macroscale variables. To highlight the general method and a computationally efficient reduction, we now discuss [15], [13], and [3] in more detail.

In [15], the authors consider the problem of deriving homogenized equations to determine the electric potential within a beating heart, where the time-dependent microstructure is close to spatially periodic in general curvilinear coordinates. Thus, the microscale may vary spatially over the macroscale. The authors transform the microscale to a strictly periodic domain, and then perform an asymptotic homogenization via the method of multiple scales on the transformed problem. The transformation of the microscale means that the derived cell problem involves coefficients from the Jacobian matrix of the transformation. Therefore, unlike a problem with strict periodicity in the microscale (such as those considered in Chapter **??**), a different cell problem must now be solved at every point in the macroscale rather than just once for the entire problem. Although this procedure is less computationally expensive than solving the full problem, there is still a significant computational expense associated with solving many different cell problems.

In [13], the dynamics of colloids suspended within a fluid moving past circular obstacles in a square array are homogenized and cell problems are derived. The colloidal particles are allowed to diffuse, advect, interact with one another due to a general interaction potential, and are allowed to attach and detach to and from the obstacles. Thus, the microstructure is not strictly periodic and the level set method is used to homogenize the problem. Although the obstacle variation is constrained to a one-parameter family, the strong coupling between the flow and colloid particle problems means that a different cell problem must be solved at every point in

the macroscale for each time step, and there remains an appreciable computational expense.

One way to reduce the cost of solving many different cell problems is to constrain the problem so that there are a limited number of possible cell problems to solve. This is the route taken in [3], where the authors consider the problem of deriving homogenized equations to the diffusion equation in a domain obstructed by nonoverlapping impermeable spheres whose centres are located on a periodic lattice. The radius of adjacent spheres is allowed to vary by an amount that is small compared to the separation of sphere centres. Defining the separation of sphere centres as the microscale length and the slow variation of sphere radius as the macroscale length, this set-up allows for a macroscale variation in microstructure. Importantly, this variation is constrained to a one-parameter family: the sphere radius. Thus, although one must still solve several cell problems to yield the homogenized problem, the range of possible cell problems only involves varying one parameter. Therefore, the general homogenized problem can be fully characterized by solving, say, 50 cell problems, each using a different sphere radius, and interpolating the relevant data for a sphere whose radius falls between two of the calculated data points. As the sphere radius determines the solid fraction of a cell, the entire homogenized problem can be written in terms of the cell-averaged porosity. An interesting conclusion from [3] is that a porosity variation induces a macroscale advection of concentration averaged over the entire cell in the direction of decreasing porosity.

A notable difference between the main problem presented in [15] to those considered in [3, 13] is that the microstructure is strictly periodic in [15] after transformation, whereas the microstructure is only close to periodic in the latter two. Thus, the main cell problems in [15] vary due to the differing coefficients in the governing equations, whereas the main cell problems in [3, 13] vary due to their differing geometries. It is shown in [15] that one can move between these two formulations for a general transformation, and it is further shown in [3] that a conformal transformation has a simplified cell problem due to the form of the Jacobian matrix. Moreover, as noted in [3], a conformal transformation also has the property that spherical obstacles remain spherical, and thus it is relatively simple to switch between the cases of sphere centres being located on a strictly periodic lattice with varying sphere radius and sphere centres being located on a locally periodic lattice with constant sphere radius. In either case, particular care must be taken when evaluating the unit normal to the obstacle surface, which may appear in Neumann or Robin boundary conditions. Between two near-to-periodic cells, there may be a small variation in the unit normal to the obstacle surface, due to a change in the position of the surface. As emphasized in [3], this must be taken into account during the homogenization procedure.

An important modelling question is whether a regular lattice can be a good approximation of an unstructured medium that may be encountered in physical problems. This has been investigated in [6] and [3]. In [6], the steady problem of nutrient uptake past randomly placed point sinks is considered in one spatial dimension. As the governing equations can be solved if the locations of the sinks are known, significant analytic progress is made into investigating the macroscale effect of different

random distributions. The authors show that, although leading-order approximations remain the same between periodic and random microscale structure, the error terms vary in magnitude and large spatial gradients can occur from error terms in certain parameter regimes. In [3], the authors also investigate the error introduced when one treats an unstructured microstructure as near-periodic. The authors compare results for an ordered and disordered microstructure in the limit of a low fraction of obstacles. They solve the full problem in both cases, and compare these results to the solution of the homogenized problem, concluding that there is little difference between the solutions.

The method used in [3] to homogenize the diffusion equation past impenetrable spheres has been extended to consider filtration problems in a similar domain. In [7], the authors homogenize the flow past a periodic array of impermeable spheres with a near-periodic microstructure and the coupled problem of solute transport owing to advection, diffusion, and adsorption onto the surfaces of the spheres. As in [3], the near periodicity of the spheres in [7] is due to a slow spatial variation in sphere radius. The motivation of [7] is to understand why filters with gradients in porosity tend to be more effective than uniform filters, where the spherical obstacles model the filter. The authors find that filtration is significantly more uniform in filters whose porosity decreases with depth compared to uniform filters, but the average filtration tends to be similar. As a large particulate removal in one place may result in reduced pore space, it is conjectured in [7] that filters with a decreasing porosity have a longer lifespan before blocking. This conjecture is confirmed in a subsequent paper [8], where a similar problem to [7] is considered, but now the blocking effect is explicitly accounted for by allowing the spheres to grow in time according to their adsorption of particulates. Thus, the microstructure now varies both temporally and spatially. Although the system presented in [8] involves a moving boundary as in [13], the problem is simplified by exploiting the slow growth of obstacles due to slow particle accumulation compared to flow velocity, thus the range of possible cell problems only involves varying one parameter as in [3]. Using asymptotic results, the authors are able to solve the inverse problem of determining the initial porosity distribution of filters that block everywhere at once, and they show that these filters remove more particulates than other filters with the same initial average porosity. The general framework presented in [8] could also consider shrinking obstacles in, for example, chemotherapy delivery, by changing the sign of the obstacle growth term.

1.1.2 Chapter outline

In this Chapter, we consider the problem of homogenizing the concentration field of a dissolved drug that diffuses within a two-dimensional domain containing circular inclusions. The boundaries of these circles can absorb the drug, and the circle centres are arranged on a periodic square lattice. We define distances of the same order as the distance between circle centres as the *microscale*, and we allow the

sphere radii to vary spatially over a significantly larger distance that we term the *macroscale*. This set-up could model drug delivery to tissue, but we do not dwell on the physical implications of this as our main focus is on the method used to homogenize a microscale with a macroscale variation.

1.2 Model set-up

We consider a system where the concentration field of a dissolved drug evolves due to diffusion within a domain obstructed by tissue, modelled as a periodic square array of circular obstacles. The boundaries of this tissue act as sinks for the concentration field, modelling drug delivery. We start with the dimensionless problem, to allow us to focus on the homogenization procedure.

The concentration field is given by $c(\mathbf{x},t)$ (where $\mathbf{x}$ is the spatial vector coordinate and t is time), and is defined within $\Omega_f \subset \mathbb{R}^2$, outside the array of circular tissue.[1] Although we do not explicitly account for fluid flow in this Chapter (this extension is considered in [7, 8, 13]), it is helpful to refer to Ω_f as the fluid phase. We define the tissue as $\Omega_s \subset \mathbb{R}^2$, and we refer Ω_s as the solid phase. The entire domain is $\Omega = \Omega_f \cup \Omega_s \subset \mathbb{R}^2$, and we note that the fluid and solid phase are distinct, so that $\Omega_f \cap \Omega_s = \emptyset$. The circular boundaries between fluid and solid phase are defined as $\partial\Omega_f$.The tissue is modelled by a collection of fixed non-overlapping circles, whose centres are located on a square lattice at a distance ε apart, where ε is a small dimensionless parameter and the typical dimensionless macroscale length is 1. We allow the circle radii to vary in space, and a circle with centre at $\mathbf{x}$ has radius $\varepsilon R(\mathbf{x})$, where $R = O(1)$. A schematic of this set-up is given in figure 1.1.

The concentration field is governed by the standard diffusion equation with a partially absorbing Robin boundary condition:

$$\frac{\partial c}{\partial t} = \nabla^2 c, \qquad \mathbf{x} \in \Omega_f, \tag{1.1a}$$

$$-\varepsilon\gamma c = \mathbf{n}\cdot\nabla c, \qquad \mathbf{x} \in \partial\Omega_f, \tag{1.1b}$$

and we are interested in the cases where $c = O(1)$ and $t = O(1)$. Physically, the boundary condition (1.1b) states that the solute uptake on the circular boundaries (equivalently, the flux of solute into the circular obstacle) is proportional to the concentration of the drug on the tissue boundary. Here, $\varepsilon\gamma = O(\varepsilon)$ is an experimentally determined uptake coefficient that will depend on the combination of drug and tissue. As the uptake coefficient is of $O(\varepsilon)$, there is a small flux into each obstacle and this leads to a distinguished asymptotic limit in the final homogenized equation, where all mechanisms contribute at leading order. The boundary condition (1.1b) is a simple model of drug uptake on the tissue boundary, and the left-hand side can easily be generalised to a different uptake model, as long as the uptake coefficient is of $O(\varepsilon)$. For example, one could alternatively use a Michaelis–Menten type con-

[1] We note that this method can easily be extended to three dimensions, as seen in [3, 7, 8].

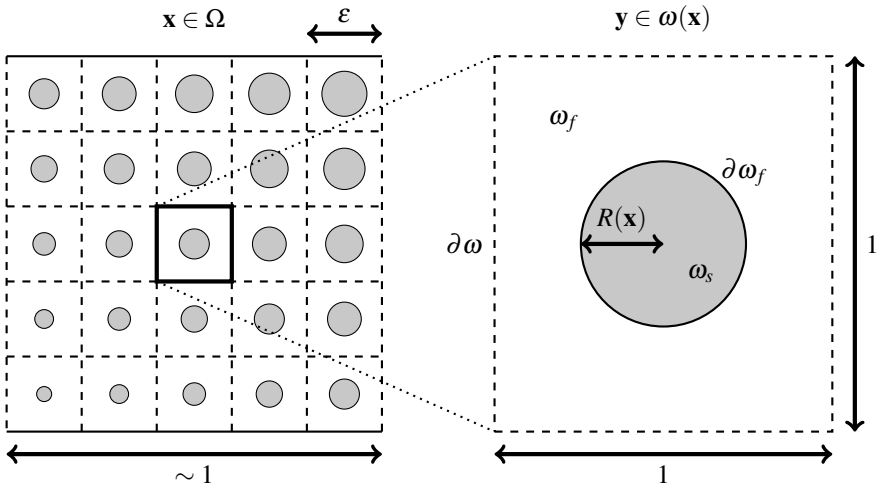

Fig. 1.1 A schematic of the model. Left: An example of a near-to-periodic set-up where the microscale varies over the macroscale. Right: A magnified view of a given cell $\omega(\mathbf{x})$, with microscale coordinate $\mathbf{y} \in \left[-\frac{1}{2}, \frac{1}{2}\right]^2$.

dition $-\varepsilon\gamma c/(K+c)$ on the left-hand side of (1.1b), where K is constant, to model saturation of uptake.

We now perform an asymptotic homogenization using the method of multiple scales on the problem defined by (1.1), exploiting the asymptotic limit $\varepsilon \to 0$. This limit corresponds to there being a small ratio of distance between adjacent circle centres and the lengthscale of the macroscale variation in circle radius.

1.3 Homogenization

To perform the asymptotic homogenization, we introduce the microscale variable $\mathbf{y} = \mathbf{x}/\varepsilon$ and treat $\mathbf{x}$ and $\mathbf{y}$ as independent. The extra degree of freedom introduced by this additional independent variable is later removed by imposing that the solution is exactly periodic in $\mathbf{y}$. Hence, any small variation between unit cells is captured through the macroscale variable $\mathbf{x}$. The microscale variable $\mathbf{y}$ is defined within a given unit cell $\omega(\mathbf{x})$, whereas the macroscale variable $\mathbf{x}$ is defined across the entire domain (figure 1.1). The tissue is denoted $\omega_s(\mathbf{x})$ and the fluid portion is $\omega_f(\mathbf{x}) = \omega(\mathbf{x}) \setminus \omega_s(\mathbf{x})$. The circular tissue–fluid boundary within the unit cell is denoted by $\partial\omega_f(\mathbf{x})$, while the square outer boundary of the unit cell is $\partial\omega(\mathbf{x})$.

We now consider each dependent variable as a function of both $\mathbf{x}$ and $\mathbf{y}$. Using the new variable $\mathbf{y}$, we transform spatial derivatives in the following manner

$$\nabla \mapsto \nabla_{\mathbf{x}} + \frac{1}{\varepsilon}\nabla_{\mathbf{y}}, \tag{1.2}$$

where $\nabla_{\mathbf{x}}$ and $\nabla_{\mathbf{y}}$ refer to the nabla operator in the $\mathbf{x}$- and $\mathbf{y}$-coordinate systems respectively.

As our eventual goal is to derive homogenized equations that are valid in the macroscale domain, it will be useful to introduce some quantities averaged over the microscale. Our eventual homogenized equations will be in terms of these averaged quantities. For this purpose, we define the cell-averaged porosity $\phi(\mathbf{x})$ to be

$$\phi(\mathbf{x}) = \frac{|\omega_f(\mathbf{x})|}{|\omega(\mathbf{x})|} = |\omega_f(\mathbf{x})|, \tag{1.3}$$

where we use the fact that $|\omega(\mathbf{x})| = 1$ in our microscale geometry to obtain the second equality. In a different microscale, for example, a hexagonal lattice rather than a square one, the cell area may be a different constant. As $\phi = 1 - \pi R^2$, we note that the cell-averaged porosity is bounded above by $1 - \pi/4$, which occurs when a circle radius is 0.5. This results in adjacent circles touching, and a subsequent change in the topology of the domain, so we restrict our domain to $0 < R < 0.5$.

There are two main ways to describe an average concentration in our problem, depending on whether the averaging takes place over the fluid phase of the cell or over the entire cell. These different averaging methods are known as the intrinsic-averaged and the volumetric-averaged concentrations, respectively. Formally, the intrinsic-averaged concentration is defined as

$$\tilde{C}(\mathbf{x},t) = \frac{1}{|\omega_f(\mathbf{x})|}\int_{\omega(\mathbf{x})} c(\mathbf{x},\mathbf{y},t)\,\mathrm{d}\mathbf{y} = \frac{1}{\phi(\mathbf{x})}\int_{\omega_f(\mathbf{x})} c(\mathbf{x},\mathbf{y},t)\,\mathrm{d}\mathbf{y}, \tag{1.4a}$$

and the volumetric-averaged concentration is defined as

$$C(\mathbf{x},t) = \frac{1}{|\omega(\mathbf{x})|}\int_{\omega(\mathbf{x})} c(\mathbf{x},\mathbf{y},t)\,\mathrm{d}\mathbf{y} = \int_{\omega_f(\mathbf{x})} c(\mathbf{x},\mathbf{y},t)\,\mathrm{d}\mathbf{y}, \tag{1.4b}$$

imposing that $c \equiv 0$ in $\omega_s(\mathbf{x})$.

1.3.1 Transforming the normal

A key consideration in homogenizing a problem whose microscale structure varies in the macroscale is the form of the unit normal. Thus, this is not an issue when a problem has Dirichlet boundary conditions. However, for Neumann or, as in our problem, Robin boundary conditions, we must take care with the unit normal to the tissue boundary. This is carried out by considering a level set function, as used in [9, 14, 17, 18] for a general obstacle shape, and in [3, 7, 8] for the specific case of a circular obstacle.

To derive the unit normal, we introduce the scalar function

$$\chi(\mathbf{x},\mathbf{y}) = R(\mathbf{x}) - \|\mathbf{y}\|, \tag{1.5}$$

where $\chi(\mathbf{x},\mathbf{y}) = 0$ defines the tissue–fluid interface in a cell. Then, the normal vector $\mathbf{n}$ in (1.1b) becomes

$$\mathbf{n} = \frac{\nabla\chi}{\|\nabla\chi\|} = \frac{\mathbf{n}_\mathbf{y} + \varepsilon\nabla_\mathbf{x} R}{\|\mathbf{n}_\mathbf{y} + \varepsilon\nabla_\mathbf{x} R\|}, \tag{1.6}$$

where the second equality arises from the gradient transform (1.2), $\mathbf{n}_\mathbf{y} = -\mathbf{y}/\|\mathbf{y}\|$ is the outward unit normal on the obstacle boundary $\partial\omega_f(\mathbf{x})$, and $\varepsilon\nabla_\mathbf{x} R$ accounts for the macroscale effect of varying obstacle size. This latter term is unexpected, but we will see later that it is vital in tracking how adjacent cells vary.

Before we carry on with the homogenization procedure, we note that $\mathbf{x}$ varies by an $O(\varepsilon)$ amount across one cell. We show in Appendix 1 that switching between a small variation in $\mathbf{x}$ across one cell and taking $\mathbf{x}$ to be constant within one cell does not affect our analysis. It should be noted, however, that this small variation is an issue if there is an integral constraint in the problem, even for a strictly periodic microscale [4].

1.3.2 Homogenization procedure

Using the transformations (1.2) and (1.6), the solute-transport problem (1.1) in one cell is

$$\varepsilon^2\frac{\partial c_0}{\partial t} = (\nabla_\mathbf{y} + \varepsilon\nabla_\mathbf{x})\cdot((\nabla_\mathbf{y} + \varepsilon\nabla_\mathbf{x})\,c), \qquad \mathbf{y}\in\omega_f(\mathbf{x}), \tag{1.7a}$$

$$-\varepsilon^2\gamma c = (\mathbf{n}_\mathbf{y} + \varepsilon\nabla_\mathbf{x} R)\cdot((\nabla_\mathbf{y} + \varepsilon\nabla_\mathbf{x})\,c) + O(\varepsilon^3), \qquad \mathbf{y}\in\partial\omega_f(\mathbf{x}), \tag{1.7b}$$

$$c \text{ periodic}, \qquad \mathbf{y}\in\partial\omega(\mathbf{x}). \tag{1.7c}$$

The homogenization procedure entails investigating the system (1.7) by looking for an asymptotic solution in the limit as $\varepsilon\to 0$. That is, we look for a solution to c in terms of an asymptotic expansion

$$c(\mathbf{x},\mathbf{y},t) = c_0(\mathbf{x},\mathbf{y},t) + \varepsilon c_1(\mathbf{x},\mathbf{y},t) + \varepsilon^2 c_2(\mathbf{x},\mathbf{y},t) + O(\varepsilon^3), \tag{1.8}$$

and use the method of multiple scales to derive solvability conditions for c_0. These will be in terms of the macroscale variable $\mathbf{x}$ and will yield the homogenized equations for which we are looking. Although our main interest is in c_0, we will see that we need to proceed to terms of $O(\varepsilon^2)$ to derive the solvability conditions for c_0.

1.3.2.1 The $O(1)$ problem

Substituting the asymptotic expansion (1.8) into the system (1.7) and equating powers of ε, the $O(1)$ terms yield the problem

$$0 = \nabla_{\mathbf{y}}^2 c_0, \qquad \mathbf{y} \in \omega_f(\mathbf{x}), \tag{1.9a}$$

$$0 = \mathbf{n}_{\mathbf{y}} \cdot \nabla_{\mathbf{y}} c_0, \qquad \mathbf{y} \in \partial\omega_f(\mathbf{x}), \tag{1.9b}$$

$$c_0 \text{ periodic}, \qquad \mathbf{y} \in \partial\omega(\mathbf{x}). \tag{1.9c}$$

The system (1.9) can be solved by a c_0 that is independent of $\mathbf{y}$, and the linearity of (1.9) allows us to deduce that this solution is unique. We can therefore deduce that c_0 is independent of the microscale, *i.e.* $c_0 = c_0(\mathbf{x},t)$, and this will be useful in simplifying the systems that arise from the $O(\varepsilon)$ and $O(\varepsilon^2)$ problems.

1.3.2.2 The $O(\varepsilon)$ problem

Substituting the asymptotic expansion (1.8) into the system (1.7) and equating powers of ε, the $O(\varepsilon)$ terms yield the problem

$$0 = \nabla_{\mathbf{y}}^2 c_1, \qquad \mathbf{y} \in \omega_f(\mathbf{x}), \tag{1.10a}$$

$$-\mathbf{n}_{\mathbf{y}} \cdot \nabla_{\mathbf{x}} c_0 = \mathbf{n}_{\mathbf{y}} \cdot \nabla_{\mathbf{y}} c_1, \qquad \mathbf{y} \in \partial\omega_f(\mathbf{x}), \tag{1.10b}$$

$$c_1 \text{ periodic}, \qquad \mathbf{y} \in \partial\omega(\mathbf{x}). \tag{1.10c}$$

Although we cannot solve the system (1.10) analytically, we can derive a solvability condition by integrating (1.10a) over $\omega_f(\mathbf{x})$ and using the boundary conditions (1.10b)–(1.10c). However, the solvability condition we obtain from this is just

$$-\nabla_{\mathbf{x}} c_0 \cdot \oint_{\partial\omega_f(\mathbf{x})} \mathbf{n}_{\mathbf{y}} \, \mathrm{d}s = 0, \tag{1.11}$$

where $\mathrm{d}s$ denotes the differential element of the obstacle boundary $\partial\omega_f(\mathbf{x})$, and we are able to take c_0 outside the integral because it is independent of $\mathbf{y}$. As (1.11) is trivially satisfied for any closed obstacle, we are not yet able to form a macroscale equation for c_0.

It will be useful to determine c_1 from (1.10) for use in the solvability condition we derive in the $O(\varepsilon^2)$ problem. We could do this numerically for any given function c_0, but this relies on us knowing c_0, which is the function for which we are trying to solve. Alternatively, we can note that we just require knowledge of how c_1 behaves as a function of c_0. To do this, we note that the system (1.10) is linear in c_1, and we can therefore write c_1 as the dot product of some vector function $\boldsymbol{\Gamma}$ to be determined, and $\nabla_{\mathbf{x}} c_0$, as follows

$$c_1(\mathbf{x},\mathbf{y},t) = -\boldsymbol{\Gamma}(\mathbf{x},\mathbf{y}) \cdot \nabla_{\mathbf{x}} c_0(\mathbf{x},t). \tag{1.12}$$

This allows us to reduce the problem of determining c_1 in terms of c_0 to solving the following cell problem

$$0 = \nabla_{\mathbf{y}}^2 \Gamma_i, \qquad \mathbf{y} \in \omega_f(\mathbf{x}), \tag{1.13a}$$

$$n_{y,i} = \mathbf{n}_{\mathbf{y}} \cdot \nabla_{\mathbf{y}} \Gamma_i, \qquad \mathbf{y} \in \partial\omega_f(\mathbf{x}), \tag{1.13b}$$

$$\Gamma_i \text{ periodic}, \qquad \mathbf{y} \in \partial\omega(\mathbf{x}), \tag{1.13c}$$

where Γ_i is the ith component of $\boldsymbol{\Gamma}$, and $n_{y,i}$ is the ith component of the unit vector $\mathbf{n}_{\mathbf{y}}$. For the circular boundaries we are considering, we have $n_{y,i} = -y_i/R(\mathbf{x})$, where y_i is the ith component of the microscale variable $\mathbf{y}$. In practice, $\boldsymbol{\Gamma}$ can be determined by using a finite element software package.

1.3.2.3 The $O(\varepsilon^2)$ problem

In our homogenization calculations, we have not yet used the fact that the microstructure is *near* periodic rather than *strictly* periodic. This is because the $O(\varepsilon)$ correction to the normal in (1.6) has not yet appeared in our calculations. In this section, the macroscale variation in the microstructure finally imposes an effect.

Substituting the asymptotic expansion (1.8) into the system (1.7) and equating powers of ε, the $O(\varepsilon^2)$ terms yield the problem

$$\frac{\partial c_0}{\partial t} = \nabla_{\mathbf{y}} \cdot (\nabla_{\mathbf{y}} c_2 + \nabla_{\mathbf{x}} c_1) + \nabla_{\mathbf{x}} \cdot (\nabla_{\mathbf{y}} c_1 + \nabla_{\mathbf{x}} c_0), \qquad \mathbf{y} \in \omega_f(\mathbf{x}), \tag{1.14a}$$

$$-\gamma c_0 = \mathbf{n}_{\mathbf{y}} \cdot (\nabla_{\mathbf{y}} c_2 + \nabla_{\mathbf{x}} c_1) + \nabla_{\mathbf{x}} R \cdot (\nabla_{\mathbf{y}} c_1 + \nabla_{\mathbf{x}} c_0), \qquad \mathbf{y} \in \partial\omega_f(\mathbf{x}), \tag{1.14b}$$

$$c_2 \text{ periodic}, \qquad \mathbf{y} \in \partial\omega(\mathbf{x}). \tag{1.14c}$$

As with (1.10), we cannot solve the system (1.14) analytically. Rather, we are interested in obtaining a solvability condition from (1.14), and this will yield our homogenized equation for c_0.

We can derive a solvability condition by integrating (1.14a) over ω_f to obtain

$$\int_{\omega_f(\mathbf{x})} \frac{\partial c_0}{\partial t} \, \mathrm{d}\mathbf{y} = \oint_{\partial\omega_f(\mathbf{x})} \mathbf{n}_{\mathbf{y}} \cdot (\nabla_{\mathbf{y}} c_2 + \nabla_{\mathbf{x}} c_1) \, \mathrm{d}s + \int_{\omega_f(\mathbf{x})} \nabla_{\mathbf{x}} \cdot (\nabla_{\mathbf{y}} c_1 + \nabla_{\mathbf{x}} c_0) \, \mathrm{d}\mathbf{y}, \tag{1.15}$$

where the first term on the right-hand side of (1.15) has been obtained by using the divergence theorem and applying the boundary condition (1.14c).

The integrand on the left-hand side of (1.15) is independent of $\mathbf{y}$, and so can be integrated immediately. The first term on the right-hand side of (1.15) can be turned into a function of c_0 and c_1 by using the boundary condition (1.14b). Thus, we can re-write (1.15) as

$$|\omega_f(\mathbf{x})|\frac{\partial c_0}{\partial t} = \int_{\omega_f(\mathbf{x})} \nabla_{\mathbf{x}}\cdot(\nabla_{\mathbf{y}}c_1+\nabla_{\mathbf{x}}c_0)\,\mathrm{d}\mathbf{y} - \oint_{\partial\omega_f(\mathbf{x})} \nabla_{\mathbf{x}}R\cdot(\nabla_{\mathbf{y}}c_1+\nabla_{\mathbf{x}}c_0)\,\mathrm{d}s - \oint_{\partial\omega_f(\mathbf{x})} \gamma c_0\,\mathrm{d}s, \tag{1.16}$$

where we have rearranged the terms on the right-hand side.

The last term on the right-hand side of (1.16) is independent of $\mathbf{y}$, and so can be integrated immediately. The first two terms on the right-hand side of (1.16) can be simplified using the transport theorem (discussed in Appendix 2), and we can therefore write (1.16) as

$$|\omega_f(\mathbf{x})|\frac{\partial c_0}{\partial t} = \nabla_{\mathbf{x}}\cdot\int_{\omega_f(\mathbf{x})}(\nabla_{\mathbf{y}}c_1+\nabla_{\mathbf{x}}c_0)\,\mathrm{d}\mathbf{y} - \gamma|\partial\omega_f(\mathbf{x})|c_0. \tag{1.17}$$

Our solvability condition is almost solely in terms of c_0, as we require. The final step is to use the result (1.12) to write $\nabla_{\mathbf{y}}c_1$ in terms of c_0, deducing that

$$\nabla_{\mathbf{y}}c_1 = \mathrm{J}_{\boldsymbol{\Gamma}}^T\nabla_{\mathbf{x}}c_0, \tag{1.18a}$$

where $\mathrm{J}_{\boldsymbol{\Gamma}}^T$ is the transpose of the Jacobian matrix of $\boldsymbol{\Gamma}$, which is given by

$$\mathrm{J}_{\boldsymbol{\Gamma}} = \begin{pmatrix} \frac{\partial\Gamma_1}{\partial y_1} & \frac{\partial\Gamma_1}{\partial y_2} \\ \frac{\partial\Gamma_2}{\partial y_1} & \frac{\partial\Gamma_2}{\partial y_2} \end{pmatrix}, \tag{1.18b}$$

where $\boldsymbol{\Gamma}$ can be obtained by solving the cell problem (1.13).

We can use the fact that $c_0 = c_0(\mathbf{x},t)$ and (1.18) to write (1.17) as

$$|\omega_f(\mathbf{x})|\frac{\partial c_0}{\partial t} = \nabla_{\mathbf{x}}\cdot\left(\left(\int_{\omega_f(\mathbf{x})}(\mathrm{I}-\mathrm{J}_{\boldsymbol{\Gamma}}^T)\,\mathrm{d}\mathbf{y}\right)\nabla_{\mathbf{x}}c_0\right) - \gamma|\partial\omega_f(\mathbf{x})|c_0, \tag{1.19}$$

where I is the 2×2 identity matrix. We now have a solvability equation for c_0, and can transform this into the leading-order homogenized equation for the intrinsic-averaged and volumetric-averaged concentrations.

1.3.2.4 The homogenized equations

We see from (1.4) that, at leading order, intrinsic-averaged concentration is $\tilde{C}(\mathbf{x},t)\sim c_0(\mathbf{x},t)$ and the volumetric-averaged concentration is $C(\mathbf{x},t)\sim\phi(\mathbf{x})c_0(\mathbf{x},t)$. After a final rearrangement of (1.19), using $|\omega_f(\mathbf{x})| = \phi(\mathbf{x})$ from (1.3), converting functions of $\mathbf{x}$ into functions of $\phi(\mathbf{x})$ for convenience, and suppressing the argument for brevity, we obtain the homogenized equation for the intrinsic-averaged concentration

$$\frac{\partial \tilde{C}}{\partial t} = \frac{1}{\phi}\nabla_{\mathbf{x}}\cdot\left(\phi D(\phi)\nabla_{\mathbf{x}}\tilde{C}\right) - k(\phi)\tilde{C}. \tag{1.20}$$

Noting that $\phi = \phi(\mathbf{x})$, so we cannot bring factors of ϕ unchanged through a derivative, the homogenized equation for the volumetric-averaged concentration is

$$\frac{\partial C}{\partial t} = \nabla_{\mathbf{x}}\cdot\left[D(\phi)\left(\nabla_{\mathbf{x}}C - \frac{\nabla_{\mathbf{x}}\phi}{\phi}C\right)\right] - k(\phi)C, \tag{1.21}$$

where the effective diffusion, $D(\phi)$ and the effective uptake, $k(\phi)$, are defined as

$$D(\phi) = 1 - \frac{1}{\phi}\int_{\omega_f(\phi)} \frac{\partial \Gamma_1}{\partial y_1}\,\mathrm{d}\mathbf{y}, \tag{1.22a}$$

$$k(\phi) = \gamma\frac{\sqrt{4\pi(1-\phi)}}{\phi}, \tag{1.22b}$$

and $k(\phi)$ is obtained using $|\partial\omega_f| = 2\pi R = \sqrt{4\pi(1-\phi)}$.

The effective diffusion $D(\phi)$ is a scalar rather than a matrix (as it appears in (1.19)) because the cell problems for the components of $\boldsymbol{\Gamma}$, given in (1.13), are symmetric across both the y_1- and y_2-axes. Hence, $\mathrm{J}_{\boldsymbol{\Gamma}}$ is a multiple of the identity matrix and thus we could also use $\partial\Gamma_2/\partial y_2$ as the integrand in (1.22a) instead of $\partial\Gamma_1/\partial y_1$, with the same result. We also note that D is not strictly an effective diffusion coefficient in the homogenized equation for the intrinsic-averaged concentration (1.20) because of the factor of $1/\phi$ outside the derivative and the factor of ϕ inside the derivative. The effective diffusion can be computed by solving the cell problem (1.13) for a given cell porosity ϕ, which is determined by the radius of the circular obstacle. We do this numerically using the finite-element software Comsol MULTIPHYSICS. The effective diffusion monotonically increases from 0 to 1 as the porosity increases from $1-\pi/4 \approx 0.21$ to 1 or, equivalently, as the circle radius decreases from 0.5 to 0 (figure 1.2a). As the microstructure gets closer to blocking and ϕ gets closer to $1-\pi/4$, the diffusion coefficient sharply decreases towards 0. This is because it is very difficult for a drug particle in one region to diffuse to another region when the gaps between nearly touching circles get very small.

The effective uptake $K(\phi)$ requires no further problems to be solved, as an explicit representation is given in (1.22b). The effective uptake monotonically decreases from $\pi/\sqrt{1-\pi/4} \approx 14.64$ to 0 as the porosity increases from $1-\pi/4 \approx 0.21$ to 1 or, equivalently, as the circle radius decreases from 0.5 to 0 (figure 1.2b). The effective uptake vanishes when the porosity approaches 1 because, in this limit, there is no tissue available to absorb the drug.

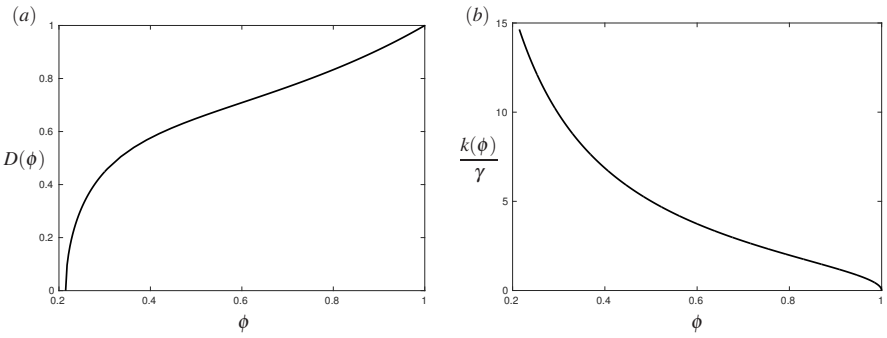

Fig. 1.2 The effective diffusion and uptake coefficients for $\phi \in (1-\pi/4, 1)$. (a) The effective diffusion $D(\phi)$. (b) The (scaled) effective uptake $k(\phi)/\gamma$. As $\phi \to (1-\pi/4)^+$, the domain tends to that of touching circles where the fluid domain becomes disconnected, and thus the effective diffusion vanishes. As $\phi \to 1^-$, the circular obstacles have a vanishingly small radius. This limit is regular, and thus the effective diffusion and uptake attain the values one would expect. That is, the effective diffusion is 1, and the effective uptake vanishes.

1.4 Interpreting the homogenized problem

The two homogenized equations (1.20) and (1.21) are equivalent through the transformation $\tilde{C}(\mathbf{x},t) = \phi(\mathbf{x})C(\mathbf{x},t)$. We discuss the implications of the homogenized problem by referring only to (1.21), the homogenized equation for the volumetric-averaged concentration, as this equation is in standard advection–diffusion–reaction form.

We see that the reaction term, which arises from the Robin boundary condition modelling uptake on the boundary in the full problem, now appears as a bulk uptake, weighted by the boundary length to fluid phase area in a cell. This bulk term is one that we may have anticipated from the start.

Perhaps more surprisingly, the macroscale variation of the porosity has resulted in the presence of an advection term in the direction of a negative porosity gradient, as identified in [3, 7, 8]. This term advects the dissolved drug towards regions of larger porosity, and can be understood by noting that (1.21), the homogenized equation, is an equation for the concentration averaged over the *entirety* of one cell, including the tissue phase. Thus, as the area of the fluid phase is greater within cells with a larger porosity, the intrinsic smoothing of diffusion will act to increase the concentration averaged over an entire cell in cells with a larger porosity.

We additionally note that when the cell-averaged porosity is constant, and there is no macroscale variation in the microscale, the homogenized equations for the intrinsic-averaged and volumetric-averaged concentrations (1.20)–(1.21) reduce to the result that could be obtained from a traditional homogenization procedure with a strictly periodic microscale.

Appendix 1

When carrying out a homogenization using the method of multiple scales, the variation of the macroscale variable x across one cell is often ignored, and x is treated as a constant when the microscale variable varies (this microscale variable can be formally defined as $y = x/\varepsilon - \lfloor x/\varepsilon \rfloor$). Note that we just consider a one-dimensional problem in this Appendix, but the argument we present generalizes to higher dimensions.

If there is a boundary condition or a boundary within a cell that depends on x and y, this should vary slowly with x through a cell. In this section, we see that it is fine to treat x as a constant when prescribing a boundary or for a Robin boundary condition. Note that this is *not* true for integral constraints, and the reasons for this are investigated in [4]. We first show that it is fine to treat x as a constant within one cell when working with a boundary that depends on x and y, then show that the Robin boundary condition is also unchanged.

Consider a problem where the boundary is defined as

$$f(x,y) = 0 \tag{1.23}$$

within a cell. Then, using the asymptotic expansion $f = f_0 + \varepsilon f_1 + \cdots$, writing $x = x_0 + \varepsilon y$, where $x_0 = \varepsilon \lfloor x/\varepsilon \rfloor$, and expanding the first argument in a Taylor series, we obtain

$$f(x_0 + \varepsilon y, y) = \sum_{m=0}^{\infty} \varepsilon^m \sum_{n=0}^{m} y^n \frac{\partial^n f_{m-n}}{\partial x^n}(x_0, y) = 0. \tag{1.24}$$

Note that we can change x_0 by an $O(\varepsilon)$ amount (that is, evaluate x_0 anywhere within a cell), and (1.24) remains unchanged when evaluating $f(x,y)$.

We proceed by showing $f_i(x_0,y) = 0$ for all $i \geqslant 0$ by induction, and hence that the $O(\varepsilon^i)$ perturbation to the interface is the same if we perturb x by $O(\varepsilon)$. Namely, that it does not matter where we evaluate the macroscale variable within a cell.

The result for $i = 0$ follows from the $O(1)$ equation. The $O(\varepsilon^I)$ equation is

$$\sum_{n=0}^{I} y^n \frac{\partial^n f_{I-n}}{\partial x^n}(x_0, y) = 0. \tag{1.25}$$

Under the induction assumption, that $f_i(x_0,y) = 0$ for all integers i such that $0 \leq i \leq I-1$, all terms apart from $n = 0$ vanish immediately, yielding

$$f_I(x_0, y) = 0, \tag{1.26}$$

as required, thus showing that $f_i(x_0,y) = 0$ for all integers $i \geqslant$, and that we can evaluate the macroscale variable anywhere within a cell when defining a boundary.

We now consider a general Robin boundary condition

$$u'(x,y) + \alpha u(x,y) + \beta = 0. \tag{1.27}$$

Under the multiple scales transformation, where $\partial_x \mapsto \partial_x + \varepsilon^{-1}\partial_y$, using the asymptotic expansion $u = u_0 + \varepsilon u_1 + \cdots$, and writing $u(x,y) = u(x_0 + \varepsilon y, y)$, the Robin boundary condition (1.27) becomes

$$\sum_{m=0}^{\infty} \varepsilon^m \sum_{n=0}^{m} y^n \left(\frac{\partial^{n+1} u_{m-n}}{\partial y \partial x^n} + \varepsilon \left(\frac{\partial^{n+1} u_{m-n}}{\partial x^{n+1}} + \alpha \frac{\partial^n u_{m-n}}{\partial x^n} \right) \right) + \varepsilon\beta = 0, \qquad (1.28)$$

evaluated at (x_0, y).

Our induction hypothesis is that the standard multiple scales transformation and asymptotic expansion for u will be valid no matter where we evaluate x within a cell. That is, we wish to show that $\partial_y u_i(x_0,y) + \partial_x u_{i-1}(x_0,y) + \alpha u_{i-1}(x_0,y) + \beta\delta_{1i} = 0$ for all integers $i \geqslant 0$, where $u_j \equiv 0$ for $j < 0$, and δ_{kl} is the Kronecker delta.

The result for $i = 0$ follows from the $O(1)$ equation. The $O(\varepsilon^I)$ equation is

$$\sum_{n=0}^{I} y^n \frac{\partial^n}{\partial x^n} \left(\frac{\partial u_{I-n}}{\partial y} + \frac{\partial u_{I-n-1}}{\partial x} + \alpha u_{I-n-1} \right) + \beta\delta_{1I} = 0, \qquad (1.29)$$

evaluated at (x_0, y). Under the induction hypothesis, $\partial_y u_i + \partial_x u_{i-1} + \alpha u_{i-1} + \beta\delta_{1i} = 0$ at (x_0, y) for all integers i such that $0 \leq i \leq I-1$, all terms inside the sum apart from the $n = 0$ term vanish, leaving

$$\frac{\partial u_I}{\partial y} + \frac{\partial u_{I-1}}{\partial x} + \alpha u_{I-1} + \beta\delta_{1I} = 0, \qquad (1.30)$$

evaluated at (x_0, y), as required. Thus, we have shown that $\partial_y u_i + \partial_x u_{i-1} + \alpha u_{i-1} + \beta\delta_{1i} = 0$ at (x_0, y) for all integers $i \geqslant 0$, and that we can evaluate the macroscale variable anywhere within a cell when using a Robin boundary condition.

Finally, note that we have written $R(\mathbf{x})$ in (1.5) as a continuous function of the macroscale variable $\mathbf{x}$, rather than a piecewise constant function evaluated at the centre of the relevant unit cell. This simplifies the subsequent analysis while affecting only the boundary condition (1.7b) at higher orders than we need to consider. As a result, our final leading-order macroscale equation (1.21) is unchanged by employing this simplification.

Appendix 2

The transport theorem allows one to differentiate through an integral where the domain of integration depends on the variable of differentiation. In general, this yields two different terms: one from the variation of the integrand over the domain, and another from the variation of the domain with respect to the variable of integration. The transport theorem is often used to calculate derivatives with respect to time, and hence the second term often involves the velocity of the boundary. However, we are interested in the derivative with respect to space. In particular, with respect to the macroscale variable $\mathbf{x}$.

We note that any variation between two different fluid regions $\omega_f(\mathbf{x}_1)$ and $\omega_f(\mathbf{x}_2)$ is due to the difference in the radius of the circle within each cell, given by $R(\mathbf{x}_1)$ and $R(\mathbf{x}_2)$, respectively, and is not affected by the outer boundary, given by $\omega(\mathbf{x}_1)$ and $\omega(\mathbf{x}_2)$, respectively. Moreover, the rate of change of the circle $\omega_s(\mathbf{x}) = \omega(\mathbf{x}) \setminus \omega_f(\mathbf{x})$ with respect to $\mathbf{x}$ is $\nabla_{\mathbf{x}} R$. This can be deduced by considering the difference over the domains $\omega_f(\mathbf{x})$ and $\omega_f(\mathbf{x}+\xi\mathbf{e}_i)$ as $\xi \to 0$, where $\mathbf{e}_i$ is the unit vector in the direction of increasing x_i. The resulting domain of integration is a shell whose thickness is approximately $\xi \partial R/\partial x_i$ as $\xi \to 0$. As we are considering an integral over $\omega_f(\mathbf{x}) = \omega(\mathbf{x}) \setminus \omega_s(\mathbf{x})$, the relevant velocity of the interior boundary is $-\nabla_{\mathbf{x}} R$.

Therefore, for any vector function $\mathbf{v}(\mathbf{x},\mathbf{y},t)$, the relevant transport theorem is given by

$$\nabla_{\mathbf{x}} \cdot \int_{\omega_f(\mathbf{x})} \mathbf{v}\,\mathrm{d}\mathbf{y} = \int_{\omega_f(\mathbf{x})} \nabla_{\mathbf{x}} \cdot \mathbf{v}\,\mathrm{d}\mathbf{y} - \oint_{\partial\omega_f(\mathbf{x})} \nabla_{\mathbf{x}} R \cdot \mathbf{v}\,\mathrm{d}s. \tag{1.31}$$

Here, the first term on the right-hand side of (1.31) arises from the variation of the integrand over the domain and is relatively straightforward. The second term on the right-hand side of (1.31) arises from the variation of $\omega_f(\mathbf{x})$ with respect to $\mathbf{x}$, as described in the paragraph above.

References

[1] A G Belyaev, A L Pyatnitskii, and G A Chechkin. Asymptotic behavior of a solution to a boundary value problem in a perforated domain with oscillating boundary. *Siberian Mathematical Journal*, 39(4):621–644, 1998.

[2] A Bensoussan, J-L Lions, and G Papanicolaou. *Asymptotic analysis for periodic structures*. North-Holland Publishing Company, Amsterdam, 1978.

[3] M Bruna and S J Chapman. Diffusion in spatially varying porous media. *SIAM J. Appl. Math.*, 75(4):1648–1674, 2015.

[4] S J Chapman and S E Mcburnie. Integral constraints in multiple-scales problems. *European Journal of Applied Mathematics*, 26(05):595–614, 2015.

[5] G A Chechkin and A L Piatnitski. Homogenization of boundary-value problem in a locally periodic perforated domain. *Applicable Analysis*, 71(1-4):215–235, 1999.

[6] I L Chernyavsky, L Leach, I L Dryden, and O E Jensen. Transport in the placenta: homogenizing haemodynamics in a disordered medium. *Phil. Trans. Royal Soc. A: Math., Phys. Eng. Sci.*, 369(1954):4162–4182, 2011.

[7] M P Dalwadi, I M Griffiths, and M Bruna. Understanding how porosity gradients can make a better filter using homogenization theory. *Proc. R. Soc. A*, 471(2182), 2015. doi: 10.1098/rspa.2015.0464.

[8] M P Dalwadi, M Bruna, and I M Griffiths. A multiscale method to calculate filter blockage. *arXiv preprint arXiv:1604.07204*, 2016.

[9] T Fatima, N Arab, E P Zemskov, and A Muntean. Homogenization of a reaction–diffusion system modeling sulfate corrosion of concrete in locally periodic perforated domains. *J. Eng. Math.*, 69(2-3):261–276, 2011.

[10] U Hornung. *Homogenization and porous media*, volume 6. Springer Science & Business Media, 2012.

[11] C C Mei and B Vernescu. *Homogenization methods for multiscale mechanics*. World Scientific, 2010.

[12] M A Peter and M Böhm. Multiscale modelling of chemical degradation mechanisms in porous media with evolving microstructure. *Multiscale Modeling & Simulation*, 7(4):1643–1668, 2009.

[13] N Ray, T van Noorden, F Frank, and P Knabner. Multiscale modeling of colloid and fluid dynamics in porous media including an evolving microstructure. *Transport in porous media*, 95(3):669–696, 2012.

[14] N Ray, T Elbinger, and P Knabner. Upscaling the flow and transport in an evolving porous medium with general interaction potentials. *SIAM J. Appl. Math.*, 75(5):2170–2192, 2015.

[15] G Richardson and S J Chapman. Derivation of the bidomain equations for a beating heart with a general microstructure. *SIAM J. Appl. Math.*, 71(3): 657–675, 2011.

[16] E Sánchez-Palencia. Non-homogeneous media and vibration theory. In *Lecture Notes in Physics*, volume 127. Springer-Verlag, Berlin, 1980.

[17] T L van Noorden. Crystal precipitation and dissolution in a porous medium: effective equations and numerical experiments. *Multiscale Modeling & Simulation*, 7(3):1220–1236, 2009.

[18] T L van Noorden and A Muntean. Homogenisation of a locally periodic medium with areas of low and high diffusivity.

[19] S Whitaker. *The method of volume averaging*, volume 13. Springer Science & Business Media, 1998.

Index